

# Facile synthesis of carbon-decorated single-crystalline Fe<sub>3</sub>O<sub>4</sub> nanowires and their application as high performance anode in lithium ion batteries†

Theivanayagam Muraliganth, Arumugam Vadivel Murugan and Arumugam Manthiram\*

Received (in Cambridge, UK) 10th August 2009, Accepted 8th October 2009

First published as an Advance Article on the web 22nd October 2009

DOI: 10.1039/b916376j

**A facile microwave-hydrothermal approach has been used to synthesize single-crystalline Fe<sub>3</sub>O<sub>4</sub> nanowires within 15 min at 150 °C. The Fe<sub>3</sub>O<sub>4</sub> nanowires, after decorating with carbon, exhibit excellent cyclability and rate performance when employed as an anode in lithium ion batteries.**

In the past decade, considerable attention has been drawn towards one-dimensional (1-D) nanostructures, such as nanowires, nanorods, and nanotubes, because of their high surface to volume ratio, interesting physical properties, and potential applications in a wide range of fields like optoelectronic devices, field effect transistors, chemical/biological sensors, fuel cells, solar cells, and energy storage.<sup>1</sup> Particularly, there is a growing interest in utilizing the 1-D nanostructures as electrodes in lithium-ion batteries.<sup>2,3</sup> Magnetite (Fe<sub>3</sub>O<sub>4</sub>) is an attractive anode material for next generation lithium-ion batteries because of its high capacity, eco-friendliness, natural abundance, and high electronic conductivity.<sup>3d,4</sup> However, its application in practical lithium-ion batteries is hindered due to its low rate performance arising from kinetic limitations and poor cycling stability resulting from large volume expansion occurring during cycling.

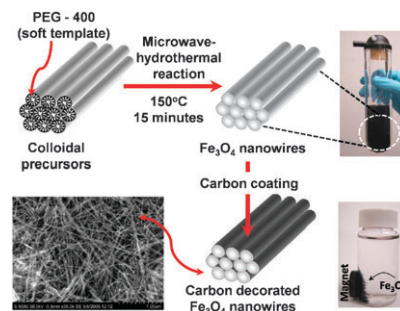
In this context, use of nanowire architectures will offer high capacity and improved cyclic stability because of their high interfacial contact area with the electrolyte and better accommodation of strain and volume change without any structural change or fracture.<sup>2,3</sup> Moreover, the 1-D nanowire morphology is beneficial for achieving high rate performance since it facilitates better electron and lithium ion transport than electrodes comprising small nanoparticles in which the electrons and lithium-ions have to move through particles and are limited by the inter-particle contacts. In this regard, development of 1-D Fe<sub>3</sub>O<sub>4</sub> nanowires can enhance the viability of Fe<sub>3</sub>O<sub>4</sub> as a high performance anode in practical lithium ion cells. Moreover, as Fe<sub>3</sub>O<sub>4</sub> is magnetic, the synthesized 1-D nanowires can have potential applications in a wide variety of fields such as data storage, magnetic resonance, gas sensors, spintronic devices, and biomedical applications.<sup>5</sup>

Various solution-based approaches, such as co-precipitation, reverse micelle, thermal decomposition, and hydrothermal methods, have been pursued in the literature for the synthesis of Fe<sub>3</sub>O<sub>4</sub> nanostructures.<sup>6</sup> Magnetite nanocrystals with

irregular morphology have also been synthesized recently by a microwave assisted sol-gel method.<sup>7</sup> However, synthesis of Fe<sub>3</sub>O<sub>4</sub> nanowires is quite complex because of its cubic crystal structure, so it requires the use of specialized templates or external applied magnetic field to orient the growth of the nanocrystals and the procedures are mostly time and energy consuming.<sup>6f-g</sup> Recently, microwave-assisted hydrothermal (MW-HT) and solvothermal (MW-ST) methods are gaining increasing popularity for nanomaterials synthesis as they offer a clean, low-cost approach to synthesize nanocrystals within a very short reaction time (in minutes) with high yields.<sup>8</sup> Herein, we report a facile MW-HT approach to synthesize Fe<sub>3</sub>O<sub>4</sub> nanowires within 15 min using polyethylene glycol (PEG-400) as a soft template in water at temperatures as low as 150 °C. The as-synthesized Fe<sub>3</sub>O<sub>4</sub> nanowires after decorating with carbon exhibit a high reversible capacity of ~830 mA h g<sup>-1</sup> with excellent cyclability and high rate performance when employed as an anode in lithium cells.

Our synthetic strategy involves the use of PEG-400 as a soft template for the synthesis of Fe<sub>3</sub>O<sub>4</sub> nanowires by the MW-HT method (see ESI† for experimental details).<sup>9</sup> The short chain polymer (PEG-400) preferentially adsorbs on the surface of a growing colloid during the synthesis, confining the colloid and facilitating anisotropic growth of the nanocrystals. The use of PEG as a soft template enables synthesis of bulk quantities of nanowires without requiring complex procedures or specialized hard templates.

Carbon coating has often been shown in recent years to improve the electrochemical performances of nanostructured anode and cathode materials due to its high electronic conductivity, good lithium permeability, and electrochemical stability.<sup>10</sup> Accordingly, the Fe<sub>3</sub>O<sub>4</sub> nanowires were decorated with carbon by a two step procedure. In the first step, the



**Scheme 1** Schematic illustration of the microwave-hydrothermal synthesis of single-crystalline Fe<sub>3</sub>O<sub>4</sub> nanowires, employing PEG-400 as a soft template and subsequent carbon decoration for application as high performance anode in lithium ion batteries.

Electrochemical Energy Laboratory, Materials Science and Engineering Program, The University of Texas at Austin, Texas, 78712, USA. E-mail: rmanth@mail.utexas.edu; Fax: (+1) 512-471-768; Tel: (+1) 512-471-1791

† Electronic supplementary information (ESI) available: Experimental details. See DOI: 10.1039/b916376j

as-synthesized  $\text{Fe}_3\text{O}_4$  nanowires were coated with glucose-derived carbon-rich polysaccharide (GCP) by sonicating with glucose solution, followed by subjecting them to the MW-HT process at  $180^\circ\text{C}$  for 15 min. Typically, hydrothermal carbonization involves an initial dehydration of the carbohydrate followed by subsequent polymerization and carbonization. It is well known that GCP can be easily carbonized and structurally ordered by heating in an inert atmosphere at lower temperatures.<sup>11</sup> Accordingly, the carbon-decorated  $\text{Fe}_3\text{O}_4$  nanowires were obtained after heating the GCP coated  $\text{Fe}_3\text{O}_4$  at  $400^\circ\text{C}$  for 3 h in Ar atmosphere. The carbon content in the composite thus obtained was determined to be  $\sim 10$  wt% from thermogravimetric analysis (TGA).

We examined the structural morphology of the as-synthesized  $\text{Fe}_3\text{O}_4$  with ultra high resolution field emission scanning electron microscopy (FE-SEM) and high resolution transmission electron microscopy (HRTEM). The representative SEM images of the as-synthesized  $\text{Fe}_3\text{O}_4$  shown in Fig. 1a and b reveal uniform nanowire-like morphology with a diameter ranging from 20 to 50 nm and a length of several micrometres. As shown in Fig. 1c, the nanowire morphology is maintained even after the MW-HT carbonization and subsequent heat treatment at  $400^\circ\text{C}$ . Fig. 1d and e show the overall view and high resolution TEM images of the carbon-decorated  $\text{Fe}_3\text{O}_4$  nanowires. The HRTEM image and fast Fourier transform (FFT) shown in Fig. 1e and f reveal that the  $\text{Fe}_3\text{O}_4$  nanowires are single crystalline and they preferentially grow along the [110] direction, which is one of the easy magnetic axes of  $\text{Fe}_3\text{O}_4$ .<sup>12</sup> Fig. 1d clearly shows the amorphous carbon nano-coating on the surface of the highly crystalline  $\text{Fe}_3\text{O}_4$  nanowire and the thickness of the carbon layer is found to be  $\sim 4$  nm.

Fig. 2a shows the XRD patterns of the as-synthesized and carbon-coated  $\text{Fe}_3\text{O}_4$  nanowires. All the reflections could be indexed on the basis of the cubic magnetite spinel phase (space group:  $Fd\bar{3}m$ ) with a lattice parameter of  $8.382 \text{ \AA}$ . The carbon-decorated  $\text{Fe}_3\text{O}_4$  did not show any impurity or peaks corresponding to carbon due to its amorphous nature or low content. Fig. 2b compares the Raman spectra of the as-synthesized and carbon-coated  $\text{Fe}_3\text{O}_4$  nanowire samples.



**Fig. 1** Morphological characterization of  $\text{Fe}_3\text{O}_4$  nanowires: (a) low and (b) high magnification FE-SEM images of as-synthesized  $\text{Fe}_3\text{O}_4$  nanowires, (c) FE-SEM image of carbon-decorated  $\text{Fe}_3\text{O}_4$  nanowires, (d) TEM and (e) HRTEM images showing crystalline  $\text{Fe}_3\text{O}_4$  nanowires surrounded by amorphous carbon, and (f) FFT image of single-crystalline  $\text{Fe}_3\text{O}_4$  nanowire. The subscript DD refers to double diffraction.

Raman spectrum of the pristine  $\text{Fe}_3\text{O}_4$  nanowire shows the characteristic peaks of magnetite at  $331$ ,  $524$  and  $670 \text{ cm}^{-1}$  that are attributed, respectively, to the  $E_g$ ,  $T_{2g}$  and  $A_{1g}$  vibrational modes,<sup>13</sup> confirming that the as-synthesized nanowires are composed of the magnetite  $\text{Fe}_3\text{O}_4$  phase. On the other hand, the Raman spectrum of the carbon-decorated  $\text{Fe}_3\text{O}_4$  nanowire shows the fundamental D and G bands for carbon at around, respectively,  $1365$  and  $1590 \text{ cm}^{-1}$  in addition to the characteristic bands for  $\text{Fe}_3\text{O}_4$ . However, the carbon spectrum could be deconvoluted into four Gaussian bands at  $1590$ ,  $1487$ ,  $1365$ , and  $1223 \text{ cm}^{-1}$ , which are referred to, respectively, as G,  $D''$ , D, and I, following the convention of Bonhomme *et al.*<sup>14</sup> used for peak fitting. The peak intensity ratio between D and G bands ( $I_D/I_G$ ) generally provides a useful index for comparing the degree of crystallinity of various carbon materials, *i.e.*, smaller the ratio of  $I_D/I_G$ , higher the degree of ordering in the carbon material. The  $I_D/I_G$  ratio was found to be 1.03, demonstrating that the carbon formed is fairly ordered, which will be beneficial for achieving better electronic conduction between adjacent nanowires.

Fig. 3a shows the first charge–discharge profiles of  $\text{Fe}_3\text{O}_4$  and carbon-decorated  $\text{Fe}_3\text{O}_4$  nanowires charged at various current rates from  $C/10$  to  $5C$  but discharged at a constant rate of  $C/10$ . For the as-synthesized  $\text{Fe}_3\text{O}_4$  nanowires, the first discharge capacity was found to be around  $1240 \text{ mA h g}^{-1}$ , corresponding to the insertion of almost 11 Li per  $\text{Fe}_3\text{O}_4$  formula. Although a small amount of capacity coming from the alloying of lithium with the copper current collector cannot be ruled out, it is usually too small to cause any significant change in the overall capacity. In the following charge, only about 8 Li could be removed reversibly resulting in a charge capacity of about  $922 \text{ mA h g}^{-1}$ . The reversible reaction occurring with lithium can be summarized as,



The initial coulombic efficiency was around 73%, which corresponds to an irreversible loss of three Li per  $\text{Fe}_3\text{O}_4$  formula. The irreversible capacity loss corresponding to three Li in the first cycle can be attributed to electrolyte reduction and formation of solid electrolyte interfacial layer (SEI). Nevertheless, after the initial cycle, the coulombic efficiency increases to above 95% in the subsequent cycles. More importantly, we are able to realize a near theoretical capacity due to the reduced lithium ion diffusion length and enhanced surface reactivity achieved because of a larger portion of atoms residing on the surface of the 1-D nanostructure and in contact with the electrolyte. However, as seen in Fig. 3b, the

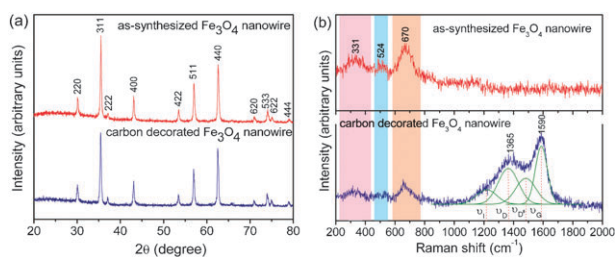


**Fig. 2** (a) X-ray diffraction and (b) Raman spectra of  $\text{Fe}_3\text{O}_4$  nanowires before and after carbon decoration.



**Fig. 3** (a) Galvanostatic charge–discharge curves of as-synthesized and carbon-decorated  $\text{Fe}_3\text{O}_4$  nanowires in lithium cells (charged at various C-rates from 0.1C to 5C but discharged at a constant rate of 0.1C) and (b) cycling performances of the  $\text{Fe}_3\text{O}_4$  nanowires before and after carbon decoration at 0.1C rate. For a comparison, data for a natural graphite electrode is also shown.

as-synthesized magnetite nanowires exhibit a gradual fade in the capacity during cycling, retaining only 50% of their initial capacity after 50 cycles. This suggests that the 1-D nanowire morphology of  $\text{Fe}_3\text{O}_4$  obtained by the MW-HT method alone is not adequate for achieving good cycle performance. Interestingly, the  $\text{Fe}_3\text{O}_4$  nanowires after decorating with carbon gives a capacity of  $\sim 830 \text{ mA h g}^{-1}$  without any capacity loss during 50 cycles. Although the initial capacity value is slightly lower than that found with the as-synthesized  $\text{Fe}_3\text{O}_4$  because of the presence of  $\sim 10 \text{ wt}\%$  inactive carbon on the surface of the  $\text{Fe}_3\text{O}_4$  nanowires, it exhibits remarkable cycling performance.

The enhanced cycling performance of the carbon-coated samples is due to the presence of the carbon buffer layer around the  $\text{Fe}_3\text{O}_4$  nanowires, preventing direct contact among the adjacent nanowires and thereby minimizing aggregation of the nanowires during electrochemical cycling. The carbon nano-coating also provides an elastic inactive matrix that can absorb the massive volume expansion and contraction occurring during charge–discharge cycling. More importantly, the carbon-decorated  $\text{Fe}_3\text{O}_4$  nanowires exhibit improved rate performance compared to the as-synthesized  $\text{Fe}_3\text{O}_4$  nanowires. For example, as seen in Fig. 3a, the carbon-decorated  $\text{Fe}_3\text{O}_4$  nanowires can still deliver a high capacity of  $600 \text{ mA h g}^{-1}$  at a high charge rate of 5C. In other words, 73% of the initial capacity could be retained at a high rate of 5C. In contrast, only 12% of the initial capacity could be retained with the as-synthesized  $\text{Fe}_3\text{O}_4$  nanowires at such a high charge rate of 5C. Herein, the improvement in rate capability is mainly attributed to the conductive carbon coating layer formed on the magnetite nanowire. Moreover, with a capacity of  $830 \text{ mA h g}^{-1}$  and with the magnetite ( $5.22 \text{ g cm}^{-3}$ ) having two times higher density than carbon ( $2.22 \text{ g cm}^{-3}$ ), the carbon decorated  $\text{Fe}_3\text{O}_4$  nanowires provide almost 5 times higher volumetric capacity than the currently used graphite anodes.

In summary, we have described a facile, rapid microwave-assisted hydrothermal synthesis approach to prepare single-crystalline  $\text{Fe}_3\text{O}_4$  nanowires and carbon-coated  $\text{Fe}_3\text{O}_4$  nanowires. The MW-HT method significantly reduces the reaction time, cost, and energy required compared to the conventional solution-based methods, and it can be employed for large scale synthesis of these technologically important magnetite

nanowires that are of interest for energy storage, data storage, spintronics devices, and biomedical applications. The  $\text{Fe}_3\text{O}_4$  nanowires after decorating with carbon provide excellent capacity retention and high rate capability when used as an anode in lithium-ion batteries. Thus, the carbon-decorated  $\text{Fe}_3\text{O}_4$  nanowires offer an attractive possibility to be used as a high capacity anode material in next generation lithium-ion batteries with high energy and power densities.

This work was supported by the Office of Vehicle Technologies of the U.S. Department of Energy under Contract No. DE-AC02-05CH11231.

## Notes and references

- (a) Y. Li, F. Qian, J. Xiang and C. M. Lieber, *Mater. Today*, 2006, **9**, 18; (b) Y. Kim, H. J. Joyce, Q. Gao, H. H. Tan, C. Jagadish, M. Paladugu, J. Zou and A. Suvorova, *Nano Lett.*, 2006, **6**, 599; (c) M. Muccini, *Nat. Mater.*, 2006, **5**, 605; (d) J. Shui and J. C. M. Li, *Nano Lett.*, 2009, **9**, 1307.
- C. K. Chan, H. Peng, G. Liu, K. Mcilwrath, X. F. Zhang, R. A. Huggins and Y. Cui, *Nat. Nanotechnol.*, 2008, **3**, 31.
- (a) A. S. Aricò, P. Bruce, B. Scrosati, W. V. Shalkwijk and J.-M. Tarascon, *Nat. Mater.*, 2005, **4**, 366; (b) Y. Wang and G. Cao, *Adv. Mater.*, 2008, **20**, 2251; (c) A. Manthiram, A. Vadivel Murugan, A. Sarkar and T. Muraliganth, *Energy Environ. Sci.*, 2008, **1**, 621; (d) P. L. Tarascon, S. Mitra, P. Poizot, P. Simon and J.-M. Tarascon, *Nat. Mater.*, 2006, **5**, 567; (e) K. T. Nam, D.-W. Kim, P. J. Yoo, C.-Y. Chiang, N. Meethong, P. T. Hammond, Y.-M. Chiang and A. M. Belcher, *Science*, 2006, **312**, 885; (f) Y. Li, B. Tan and Y. Wu, *Nano Lett.*, 2008, **8**, 265.
- (a) H. Liu, G. Wang, J. Wang and D. Wexler, *Electrochem. Commun.*, 2008, **10**, 1879; (b) S. Ito, K. Nakaoko, M. Kawamura, K. Ui, K. Fujimoto and N. Koura, *J. Power Sources*, 2005, **146**, 319.
- L. Zhang and Y. Zhang, *J. Magn. Magn. Mater.*, 2009, **321**, L15.
- (a) X. Wang, J. Zhuang, Q. Peng and Y. Li, *Nature*, 2005, **437**, 121; (b) J. Wang, Q. Chen, C. Zeng and B. Hou, *Adv. Mater.*, 2004, **16**, 137; (c) R. Fan, X. H. Chen, Z. Gui, L. Liu and Z. Y. Chen, *Mater. Res. Bull.*, 2001, **36**, 497; (d) S. Lian, Z. Kang, E. Wang, M. Jiang, C. Hu and L. Xu, *Solid State Commun.*, 2003, 127; (e) J. B. Yang, H. Xu, S. X. You, X. D. Zhou, C. S. Wang, W. B. Yelon and W. J. James, *J. Appl. Phys.*, 2006, **99**, 08Q507; (f) K. He, C. Y. Xu, L. Zhen and W.-Z. Shao, *Mater. Lett.*, 2007, **61**, 3159; (g) Z. Liu, S. Han, C. Li, B. Lei, M. P. Stewart, J. M. Tour and C. Zhou, *Nano Lett.*, 2004, **4**, 2151.
- I. Bilecka, I. Djerdj and M. Niederberger, *Chem. Commun.*, 2008, 886.
- (a) A. B. Panda, G. Glaspell and M. S. M. El-Shall, *J. Am. Chem. Soc.*, 2006, **128**, 2790; (b) J. A. Gerbec, D. Magana, A. Washington and G. F. Strouse, *J. Am. Chem. Soc.*, 2005, **127**, 15791; (c) A. Vadivel Murugan, T. Muraliganth, P. J. Ferreira and A. Manthiram, *Inorg. Chem.*, 2009, **48**, 946; (d) T. Muraliganth, A. Vadivel Murugan and A. Manthiram, *J. Mater. Chem.*, 2008, **18**, 5661.
- Z. Li, Y. Xiong and Y. Xie, *Inorg. Chem.*, 2003, **42**, 8105.
- (a) X. W. Lou, C. M. Li and L. A. Archer, *Adv. Mater.*, 2009, **21**, 2536; (b) Y.-S. Hu, R. D. Cakan, M.-M. Titirici, J.-O. Müller, R. Schlöge, M. Antonietti and J. Maier, *Angew. Chem., Int. Ed.*, 2008, **47**, 1645.
- X. M. Sun, J. F. Liu and Y. D. Li, *Chem. Mater.*, 2006, **18**, 3486.
- Y. L. Li and G. D. Li, in *Physics of Ferrites*, Science Publishing Corporation, Beijing, 1978, p. 381.
- O. N. Shebanova and P. Lazor, *J. Solid State Chem.*, 2003, **174**, 424.
- F. Bonhomme, J. C. Lassegues and L. Servant, *J. Electrochem. Soc.*, 2001, **148**(11), E450.